

Malini S. Iyer,¹ Richard N. Bergman,¹ Jeremy E. Korman,² Orison O. Woolcott,¹ Morvarid Kabir,¹ Ronald G. Victor,^{1,3} Deborah J. Clegg,¹ and Cathryn Kolka¹



Renal Denervation Reverses Hepatic Insulin Resistance Induced by High-Fat Diet



Diabetes 2016;65:3453–3463 | DOI: 10.2337/db16-0698

Activation of the sympathetic nervous system (SNS) constitutes a putative mechanism of obesity-induced insulin resistance. Thus, we hypothesized that inhibiting the SNS by using renal denervation (RDN) will improve insulin sensitivity (S_I) in a nonhypertensive obese canine model. S_I was measured using euglycemic-hyperinsulinemic clamp (EGC), before (week 0 [w0]) and after 6 weeks of high-fat diet (w6-HFD) feeding and after either RDN (HFD + RDN) or sham surgery (HFD + sham). As expected, HFD induced insulin resistance in the liver (sham 2.5 ± 0.6 vs. $0.7 \pm 0.6 \times 10^{-4} \text{ dL} \cdot \text{kg}^{-1} \cdot \text{min}^{-1} \cdot \text{pmol/L}^{-1}$ at w0 vs. w6-HFD [$P < 0.05$], respectively; HFD + RDN 1.6 ± 0.3 vs. $0.5 \pm 0.3 \times 10^{-4} \text{ dL} \cdot \text{kg}^{-1} \cdot \text{min}^{-1} \cdot \text{pmol/L}^{-1}$ at w0 vs. w6-HFD [$P < 0.001$], respectively). In sham animals, this insulin resistance persisted, yet RDN completely normalized hepatic S_I in HFD-fed animals ($1.8 \pm 0.3 \times 10^{-4} \text{ dL} \cdot \text{kg}^{-1} \cdot \text{min}^{-1} \cdot \text{pmol/L}^{-1}$ at HFD + RDN [$P < 0.001$] vs. w6-HFD, [P not significant] vs. w0) by reducing hepatic gluconeogenic genes, including G6Pase, PEPCK, and FOXO1. The data suggest that RDN downregulated hepatic gluconeogenesis primarily by upregulating liver X receptor α through the natriuretic peptide pathway. In conclusion, bilateral RDN completely normalizes hepatic S_I in obese canines. These preclinical data implicate a novel mechanistic role for the renal nerves in the regulation of insulin action specifically at the level of the liver and show that the renal nerves constitute a new therapeutic target to counteract insulin resistance.

Catheter-based renal denervation (RDN) has garnered great interest and debate as a potentially effective percutaneous

intervention to treat hypertension and related major cardiac and metabolic disorders (1,2). Destruction of these nerves interrupts both efferent renal nerves (ERNs) and afferent renal nerves (ARNs). ERNs are postganglionic sympathetic fibers that release norepinephrine (NE) and contribute to hypertension by causing renal vasoconstriction, renin release, and renal sodium and water retention (3). ARNs are sensory fibers that arise in the renal pelvis and cortex. These signal the central nervous system about changes in the chemical composition of the urine and intrarenal pressure (4) when activated by uremic metabolites such as urea, ischemic metabolites such as adenosine, or increased intrarenal pressure from excessive perinephric fat mass in animal models of obesity (5). Renal afferents can trigger sustained reflex increases in sympathetic nerve activity (SNA) targeted to multiple extrarenal tissues and vascular beds (6).

Initial enthusiasm for RDN to treat hypertension has waned after randomized sham-controlled phase III clinical trials failed to show a significant improvement in severe drug-resistant hypertension (7). However, in the early-phase trials, RDN was accompanied by reduced fasting glucose, C-peptide, and plasma insulin levels, suggesting improved insulin sensitivity (S_I) in patients with resistant hypertension (2) and in patients with hypertension and polycystic ovary syndrome (8) or obstructive sleep apnea (9). However, this putative metabolic benefit was based on indirect evidence from small uncontrolled trials. Thus, this potentially important lead has never been rigorously pursued.

We thoroughly tested the hypothesis that RDN improves S_I in a well-established nonhypertensive canine

¹Diabetes and Obesity Research Institute, Cedars-Sinai Medical Center, Los Angeles, CA

²Department of Surgery, Cedars-Sinai Medical Center, Los Angeles, CA

³Heart Institute, Cedars-Sinai Medical Center, Los Angeles, CA

Corresponding author: Malini S. Iyer, malini.s.iyer@gmail.com.

Received 1 June 2016 and accepted 26 July 2016.

This article contains Supplementary Data online at <http://diabetes.diabetesjournals.org/lookup/suppl/doi:10.2337/db16-0698/-/DC1>.

© 2016 by the American Diabetes Association. Readers may use this article as long as the work is properly cited, the use is educational and not for profit, and the work is not altered. More information is available at <http://www.diabetesjournals.org/content/license>.

model of diet-induced obesity. In vivo S_I was measured by using the minimal model approach and euglycemic-hyperinsulinemic clamp (EGC) with 3- 3 H-glucose to tease out the specific components of S_I (i.e., hepatic, peripheral) before and after 6 weeks of high-fat diet (HFD) feeding in dogs who then underwent either bilateral surgical RDN or sham surgery. Because a key unresolved limitation of catheter-based RDN clinical trials is the inability to ensure the completeness of renal nerve ablation (10,11), in this initial proof-of-concept dog study, we used a direct surgical approach to denervate renal nerves.

RESEARCH DESIGN AND METHODS

Animals

Fifteen male mongrel dogs were housed in a vivarium under controlled conditions (12:12-h light-dark cycle). Animals were included in this study only if judged to be in good health. The experimental protocol was approved by the Institutional Animal Care and Use Committee of Cedars-Sinai Medical Center. All animals had ad libitum access to water. The weight-maintaining diet (control diet) consisted of 33% fat, and the hypercaloric HFD consisted of 54% fat.

Experimental Design

Baseline assessments (week 0 [w0]) of body weight, fasting blood and urine biochemistry, and in vivo S_I were performed on all the animals while on a controlled diet. Animals were then fed an HFD for 6 weeks (w6-HFD) to induce insulin resistance as previously shown (12). The dogs were then randomized into two groups: one group underwent surgical bilateral RDN (HFD + RDN) ($n = 8$) and the other group underwent a sham operation (HFD + sham) ($n = 7$). After surgery, the animals were allowed to recover for 10 days while still being maintained on an HFD. Postsurgery metabolic assessment was performed in both groups 1 week after the animals were completely recovered from the surgery (Fig. 1A). Tissue biopsy specimens were collected at the end of postsurgery metabolic assessment. Fasting blood and urine biochemistry, body weight, and blood pressure taken with a cuff on the foreleg (SurgiVet V6004 Series Non-Invasive Blood Pressure Monitor; Smiths Medical, Norwell, MA) were assessed every week throughout the study for all the animals.

Denervation

Bilateral RDN was performed surgically and chemically. Kidneys were exposed and all the adventitial tissues were stripped. All visible nerves were surgically cut, and the stripped area was painted with 10% phenol in ethanol solution for 5 min. In the sham-operated animals, a similar surgical procedure was followed except all the visible nerves were left intact, and the renal arteries were painted with saline for 5 min.

Validation of Denervation

The efficiency and specificity of successful surgical denervation was validated by the following two methods.

Catecholamine Measurement

Tissue biopsy specimens (~200 mg) were homogenized in a buffer containing final concentrations of 1 mmol/L EDTA, 4 mmol/L sodium metabisulfite, and 0.01 N HCl, and the homogenate was centrifuged for 15 min at 3,000 rpm (4°C). The supernatant was collected and measured using 2-CAT (A-N) ELISA (Labor Diagnostika Nord, Nordhorn, Germany).

Hypoglycemic Clamp

In a subset of animals (six denervated and six sham), hypoglycemic clamp was performed before (at w6-HFD) and after denervation. Insulin (5 mU · kg⁻¹ · min⁻¹) and glucose (at variable rates, 50% dextrose, 454 mg/mL; B. Braun Medical, Melsungen, Germany) were infused to slowly decrease glycemia to ~50 mg/dL.

Assessment of S_I

In vivo S_I was assessed at w0 and w6-HFD as well as at ~3 weeks postsurgery with both EGC and the minimal model analysis as previously described (13).

Assays

Plasma from blood was collected and stored for insulin, D-3- 3 H-glucose, free fatty acids (FFAs), glycerol, and peptides as previously described (14). Assays for glucose, insulin, FFAs, glycerol, C-peptide, and glucagon were performed as previously described (12,14).

Total RNA Isolation and Real-Time PCR

RNA was extracted from tissue biopsy specimens by using the TRI Reagent Kit (Molecular Research Center, Cincinnati, OH). First-strand cDNA was synthesized using Superscript II (Invitrogen, Carlsbad, CA) from 1 μ g of total RNA. The real-time PCR was performed using Light-Cycler 4.8 (Roche Applied Science, Indianapolis, IN) according to the manufacturer's protocol.

Urine Collection and Analysis

Urine samples were collected by using a sterile one-way Foley catheter. Urine osmolality was estimated by a vapor pressure osmometer (Vapro Vapor Pressure 5520; ELITech Group, Princeton, NJ). Specific gravity of urine; urinary pH; protein-creatinine ratio; microalbuminuria; white blood cell, red blood cell, and occult blood counts; urinary tract infection; urinary casts; epithelial cells; crystals; ketones; and bilirubin were measured by Antech Diagnostics (Irvine, CA).

Statistical Analyses

Two-way repeated-measures ANOVA with Bonferroni correction was performed to compare all time course data within the groups. Student paired *t* test was used to identify the significantly different time point pairs and to compare all metabolic parameters within groups. Nonpaired *t* tests were used to compare means between groups. All analyses were performed using GraphPad InStat software (GraphPad Software, La Jolla, CA).

RESULTS

Metabolic assessments were performed at w0 (baseline prepat period), at w6-HFD, and 3 week postsurgery (HFD + sham or HFD + RDN) (Fig. 1A). At w6-HFD, body weight was increased by ~6.3% ($P < 0.001$) in the sham group and by 5.2% ($P < 0.001$) in the RDN group compared with w0 (Fig. 1B). However, neither sham nor RDN had any further effect on body weight during the time studied, and no

changes in caloric intake (except a transient increase at w2-HFD), blood pressure, and heart rate were observed with continued HFD or with surgery (Fig. 1C–E).

Validation of Denervation

We used two methods to validate the effect of the surgical technique to denervate the kidneys and differentiate the denervation from the sham surgery.

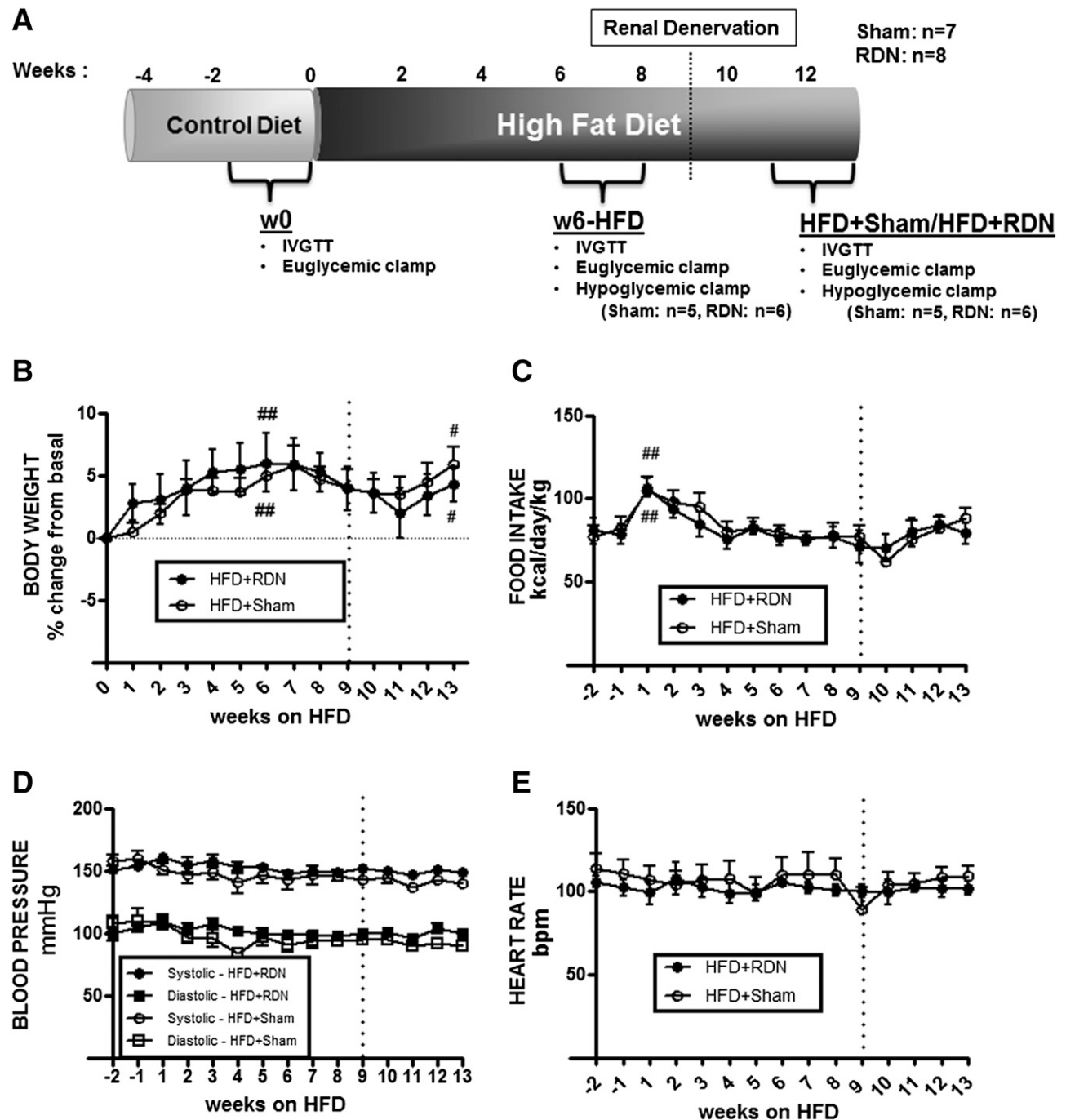


Figure 1—Experimental design (A), body weight (B), food intake (C), blood pressure (D), and heart rate (E). Vertical line represents the week of surgery. Data are mean ± SEM. ## $P < 0.001$ vs. week -1 or w0 (prepat period); # $P < 0.01$ vs. week 0 as measured by two-way ANOVA. bpm, beats/min.

Renal Catecholamine Content

Kidney cortex NE content is the most direct measurement of ERN SNA. We therefore measured NE in the renal cortex in an attempt to validate the denervation. Compared with sham animals, RDN animals had much lower NE content in the renal cortex (right-side kidney 546.4 ± 89.3 vs. 128.8 ± 36.8 ng/g, $P = 0.003$; left-side kidney 536.1 ± 88.8 vs. 196.5 ± 51.6 ng/g, $P = 0.01$) (Fig. 2A). We found analogous results with renal cortex epinephrine (EP) content (right-side kidney 11.5 ± 0.8 vs. 7.8 ± 1.2 ng/g, $P = 0.02$; left-side kidney 11.4 ± 1.2 vs. 7.5 ± 1.4 ng/g, $P = 0.09$) (Fig. 2B). It is noteworthy that renal cortical EP content was only a fraction of the total catecholamine content in the kidney. We also measured the expression of adrenergic receptors (ADRs) α -1A, α -2A, α -2B, β 1, and β 2 in the kidney. We found no difference in the ADR expression in the renal cortex (Supplementary Fig. 2), indicating that removal of neural signals from the sympathetic nerves did not affect the ADR expression in the renal cortex.

Renin Response to Hypoglycemia

The rise in plasma renin activity (PRA) in response to hypoglycemia is largely mediated by the sympathetic nervous system (SNS) (15). We studied the renin response to hypoglycemia before and after denervation. Compared with presurgery (w6-HFD), PRA during steady-state hypoglycemia (140–160 min) was modestly higher in the HFD + RDN group postsurgery, indicating higher potentiation of the renin response to hypoglycemia after RDN (RDN: basal, 2.9 ± 0.8 vs. 3.2 ± 0.9 ng · mL⁻¹ · h⁻¹ at w6-HFD vs. HFD + RDN, respectively, $P = 0.1$; steady state: 5.1 ± 1.0 vs. 6.2 ± 1.2 ng · mL⁻¹ · h⁻¹ at w6-HFD vs. HFD + RDN, respectively, $P = 0.03$) (Fig. 2D). No significant difference in PRA in response to hypoglycemia was observed in the sham group before and after surgery (sham: basal, 3.3 ± 0.8 vs. 3.0 ± 0.3 ng · mL⁻¹ · h⁻¹ at w6-HFD vs. HFD + sham, respectively, $P = 0.5$; steady state: 4.3 ± 1.4 vs. 3.9 ± 0.6 ng · mL⁻¹ · h⁻¹ at w6-HFD vs. HFD + sham, respectively, $P = 0.4$) (Fig. 2C).

Catecholamine response to hypoglycemia followed a pattern similar to PRA (Fig. 2E and F). In the HFD + RDN group, there was a tendency for greater EP response to hypoglycemia compared with w6-HFD ($P = 0.06$) (Fig. 2F). In addition to NE stimulation, renin response to hypoglycemia is controlled by circulating EP secreted by the adrenal medulla among other factors (15). The renin response to insulin-induced hypoglycemia is completely abolished only when adrenal denervation is performed in addition to RDN (16). The current results suggest, therefore, that enhanced renin response with RDN may be induced by increased adrenomedullary EP secretion during a hypoglycemic challenge. These results indicate that the surgical RDN technique was very specific and that the adrenomedullary neural circuitry was left intact.

No significant differences were found in the hypoglycemic clamp parameters, namely, baseline and steady-state glucose and insulin between the RDN and sham

groups or within groups before and after surgery (Supplementary Fig. 1A–D). Rate of glucose infusion (GINF) was significantly lower post-RDN surgery than at w6-HFD ($P < 0.0001$) (Supplementary Fig. 1F), suggesting an increased resistance to hypoglycemia with RDN, a possible protective effect against hypoglycemia. Together, the renal NE content and PRA activity during hypoglycemic challenge demonstrated that we effectively ablated only the renal nerves in RDN but not sham animals while leaving the adrenal nerves intact.

Effect of Nerve Ablation on S_I

As expected, 6 weeks of HFD reduced S_I in both the sham and the RDN groups as assessed by the minimal model (intravenous glucose tolerance test [IVGTT]) S_I: sham 7.6 ± 1.3 vs. 4.3 ± 0.5 μ U/mL⁻¹ · min⁻¹ at w0 vs. w6-HFD, respectively, $P < 0.05$; RDN 5.4 ± 0.7 vs. 2.3 ± 0.3 μ U/mL⁻¹ · min⁻¹ at w0 vs. w6-HFD, respectively, $P < 0.001$) (Fig. 3A and B) as well EGC (S_I clamp sham 13.7 ± 1.5 vs. $9.3 \pm 1.3 \times 10^{-4}$ dL · kg⁻¹ · min⁻¹ · pmol/L⁻¹ at w0 vs. w6-HFD, respectively, $P < 0.05$; RDN 9.7 ± 0.7 vs. $6.7 \pm 0.7 \times 10^{-4}$ dL · kg⁻¹ · min⁻¹ · pmol/L⁻¹ at w0 vs. w6-HFD, respectively, $P < 0.001$) (Fig. 3G). In response to the same insulin infusion rate, the rates of GINF (Fig. 3C–F) during the clamp were also significantly decreased with 6 weeks of HFD compared with baseline ($P < 0.001$) in both groups, indicating whole-body insulin resistance. Minimal model assessment of IVGTT showed that RDN partially restored HFD-impaired S_I (S_I IVGTT 3.8 ± 0.6 μ U/mL⁻¹ · min⁻¹ at HFD + RDN [$P < 0.001$] vs. w6-HFD) (Fig. 3B), but sham surgery did not (4.3 ± 0.2 μ U/mL⁻¹ · min⁻¹ at HFD + sham [P not significant] vs. w6-HFD [$P < 0.05$] vs. w0) (Fig. 3A), although these changes were not detected by S_I clamp because GINF rates were not affected by the surgery.

To identify the mechanism of improved S_I with RDN, we studied peripheral and hepatic S_I during EGC using tritiated glucose. We did not find any significant changes in R_d (Fig. 4A and B) or rate of peripheral S_I [S_I (R_d clamp)] (Fig. 4C) with HFD or surgery. Figure 4D and E show the expected loss of suppression of endogenous glucose production (EGP) with w6-HFD. This was also reflected in the reduction of S_I of EGP to insulin (hepatic insulin resistance [S_I (EGP clamp)]: sham 2.5 ± 0.6 vs. $0.7 \pm 0.6 \times 10^{-4}$ dL · kg⁻¹ · min⁻¹ · pmol/L⁻¹ at w0 vs. w6-HFD, respectively, $P < 0.05$; RDN 1.6 ± 0.3 vs. $0.5 \pm 0.3 \times 10^{-4}$ dL · kg⁻¹ · min⁻¹ · pmol/L⁻¹ at w0 vs. w6-HFD, respectively, $P < 0.001$) (Fig. 4F). RDN completely normalized liver S_I back to that at w0 despite the continuation of HFD after surgery (S_I (EGP clamp) $1.8 \pm 0.3 \times 10^{-4}$ dL · kg⁻¹ · min⁻¹ · pmol/L⁻¹ at HFD + RDN [$P < 0.001$] vs. w6-HFD, [P not significant] vs. w0; $1.0 \pm 0.3 \times 10^{-4}$ dL · kg⁻¹ · min⁻¹ · pmol/L⁻¹ at HFD + sham, [P not significant] vs. w6-HFD) (Fig. 4E and F). Renal nerve ablation totally reversed the hepatic insulin resistance induced by the HFD; sham had no such effect.

It is reasonable to assume that insulin suppression of liver EGP during clamps is due to suppression of

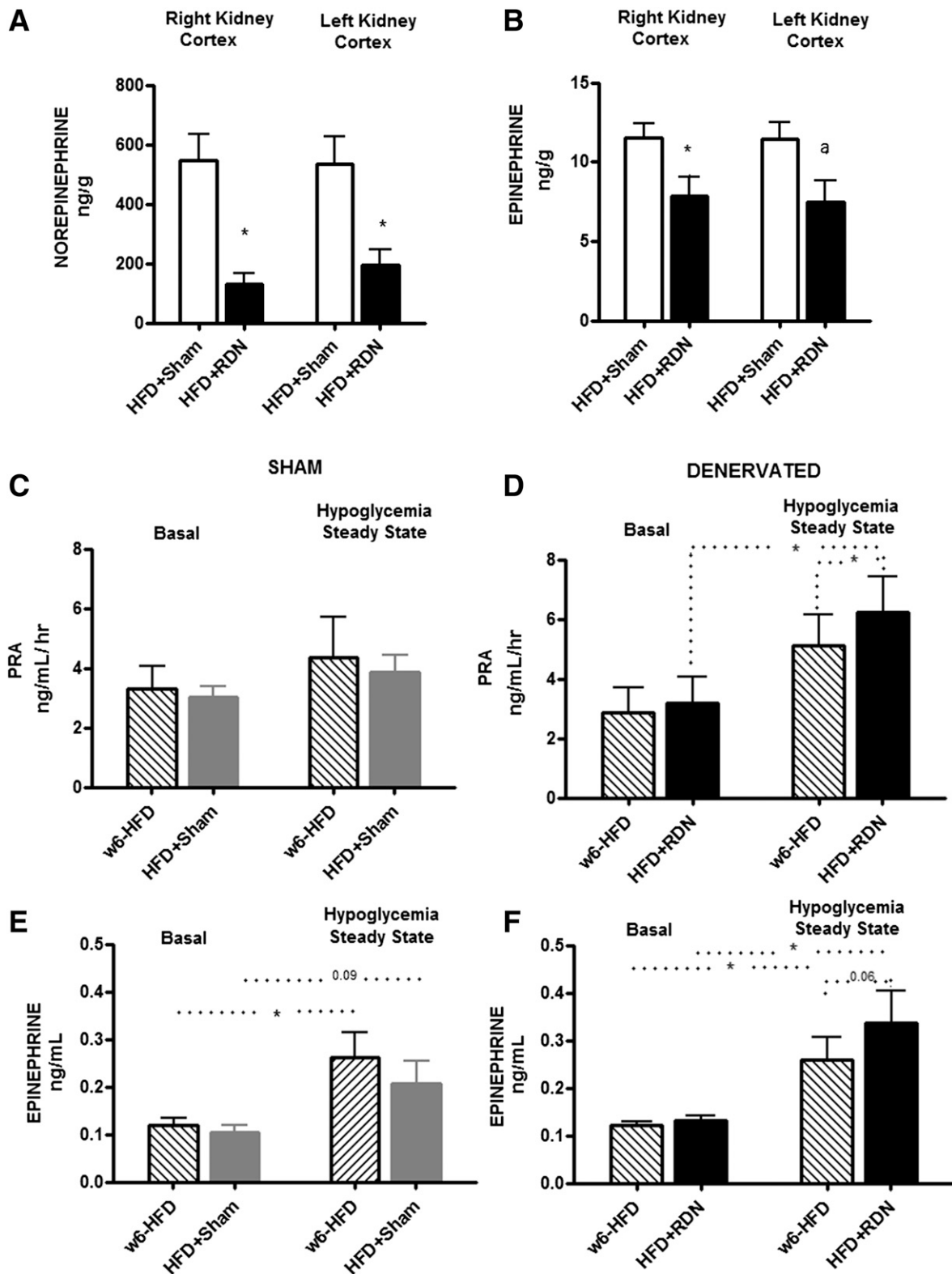


Figure 2—Validation of denervation. Renal NE (A) and EP (B) content and PRA (C and D) and plasma EP (E and F) during hypoglycemic clamp. Kidney cortex NE (A) and EP (B) content were lower in the RDN group than in the sham group, indicating successful denervation. PRA (C and D) and plasma EP (E and F) assessed during the hypoglycemic clamp show that RDN induces higher renin and EP responses to hypoglycemia than sham. Sham $n = 6$ and RDN $n = 6$. * $P < 0.05$, ^a $P = 0.09$, as measured by Mann-Whitney U nonparametric t test.

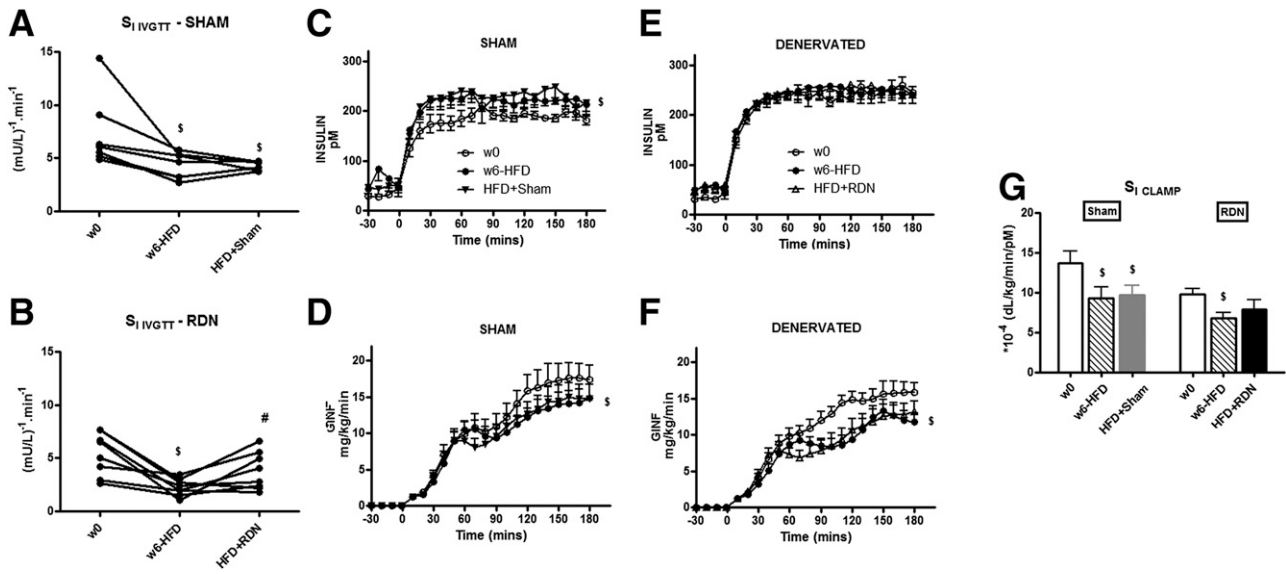


Figure 3—Whole-body S_1 measured by minimal model and EGC. *A* and *B*: S_1 IVGTT as assessed by minimal model shows that RDN surgery reverses HFD-induced insulin resistance. *C–G*: Time course data of plasma insulin concentration (*C* and *E*), GINF rate (*D* and *F*), and S_1 clamp and whole-body S_1 (*G*) as assessed during the EGC show that RDN reverses insulin resistance to EGP. Sham $n = 7$ and RDN $n = 8$. $\$P < 0.05$ vs. w0; $\#P < 0.05$ vs. w6-HFD as measured by two-way ANOVA.

gluconeogenesis. Therefore, because RDN restored liver S_1 , whether that effect is concordant with a reduction in gluconeogenic (GNG) gene expression is important. Therefore, we examined the expressions of key GNG genes in the liver and kidney. Compared with sham, the

RDN animals had significantly lower expression G6Pase (HFD + sham 0.6 ± 0.2 , HFD + RDN 0.2 ± 0.02 arbitrary units [AU], $P = 0.05$) and PEPCK (HFD + sham 0.8 ± 0.1 , HFD + RDN 0.2 ± 0.05 AU, $P = 0.01$) (Fig. 5A). We also found lower expression of transcription factors activating

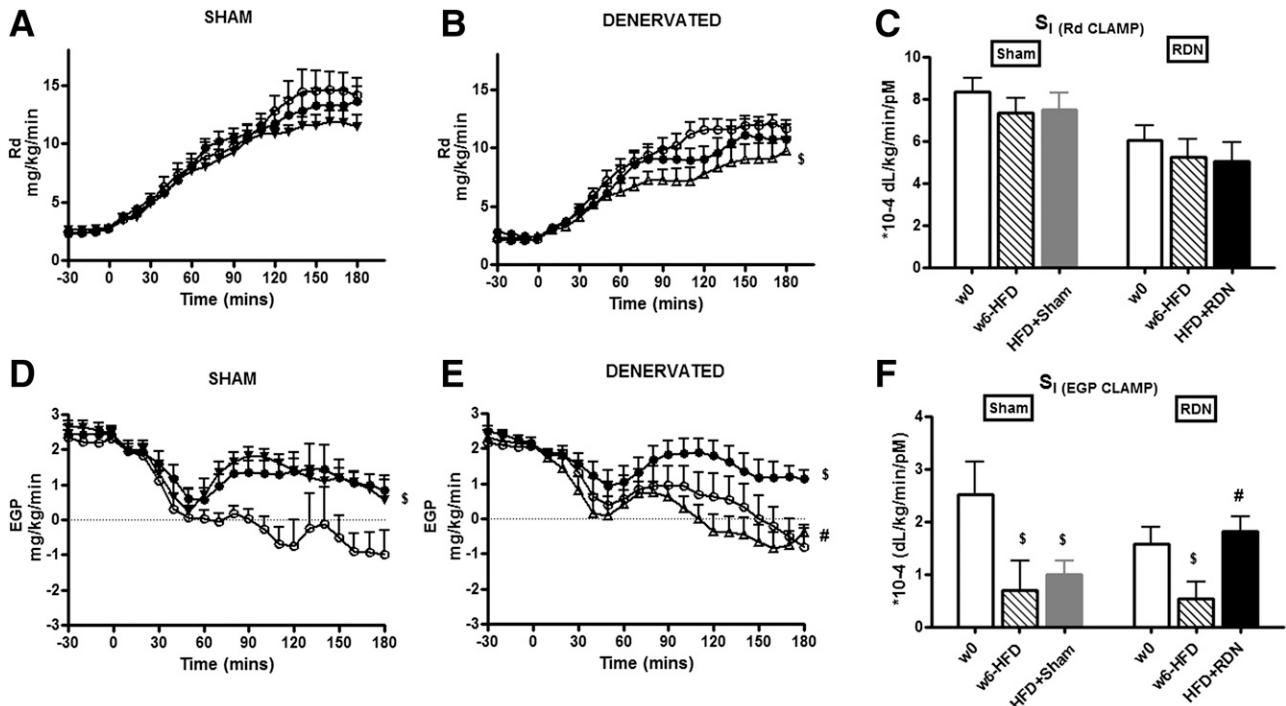


Figure 4—Peripheral and hepatic S_1 . Time course data of R_d (*A* and *B*), S_1 (R_d clamp) (*C*), peripheral S_1 and time course data of EGC (*D* and *E*), and S_1 (EGP clamp) and hepatic S_1 assessed during the EGC (*F*) show that RDN reverses insulin resistance to EGP. \circ , w0; \bullet , w6-HFD; \blacktriangledown , HFD + sham; \triangle , HFD + RDN. Sham $n = 7$ and RDN $n = 8$. $\$P < 0.05$ vs. w0; $\#P < 0.05$ vs. w6-HFD as measured by two-way ANOVA.

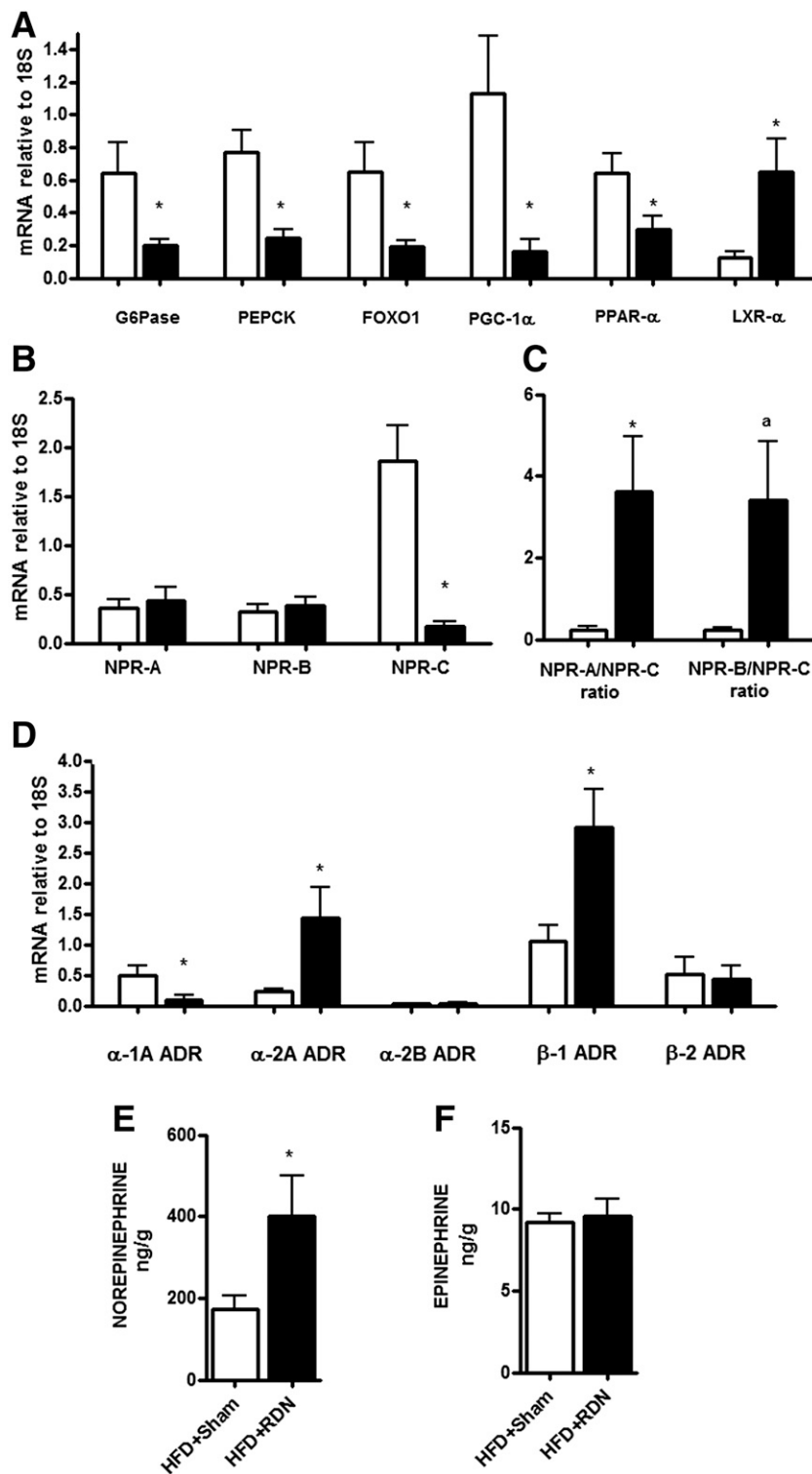


Figure 5—Expression of GNG genes (A), NPRs (B and C), ADRs (D), NE content (E), and EP content (F) in the liver. RDN reduced the expression of G6Pase, PEPCK, FOXO1, PGC-1 α , PPAR- α , and LXR- α in liver. RDN also reduced the expression of NPR-C and α -1A ADR while increasing the expression of α -2A ADR and β -1 ADR. White bars, HFD + sham ($n = 7$); black bars, HFD + RDN group ($n = 8$). Data are mean \pm SEM. * $P < 0.05$; ^a $P = 0.07$ as measured by Mann-Whitney U nonparametric t test.

GNG genes, namely FOXO1 (HFD + sham 0.6 ± 0.2 , HFD + RDN 0.2 ± 0.02 AU, $P = 0.04$), peroxisome proliferator-activated receptor γ coactivator 1 α (PGC-1 α) (HFD + sham 1.1 ± 0.3 , HFD + RDN 0.2 ± 0.05 AU, $P = 0.03$) and peroxisome proliferator-activated receptor α (PPAR- α) (HFD + sham 0.6 ± 0.1 , HFD + RDN 0.3 ± 0.1 AU,

$P = 0.03$), in the RDN animals than in the sham animals (Fig. 5A). We did not find any significant differences in the expression of G6Pase, PEPCK, and FOXO1 in the renal cortex between the two groups (Supplementary Fig. 3), suggesting that the restoration of EGP sensitivity to insulin is mainly due to the liver and not to the kidney. These data suggest that ablating the renal nerves reversed HFD-induced resistance of EGP to insulin by reducing the expression of key GNG genes primarily in the liver. Liver X receptor α (LXR- α) controls hepatic GNG genes by downregulating PGC-1 α , G6Pase, and PEPCK (17). We found that RDN greatly increased the expression of LXR- α (HFD + sham 0.1 ± 0.03 , HFD + RDN 0.7 ± 0.2 AU, $P = 0.05$) (Fig. 5A) in the liver compared with sham surgery. In a recent study, Cannon et al. (18) showed that LXR- α improves glucose tolerance in cardiomyocytes by inducing the expression of A-type and B-type natriuretic peptides. In the current model, we found that RDN reduced the expression of natriuretic peptide clearance receptor (NPR-C) (HFD + sham 1.9 ± 0.4 , HFD + RDN 0.2 ± 0.04 AU, $P = 0.001$) (Fig. 5B) but not natriuretic peptide receptor (NPR) A or NPR-B. This indicates that RDN surgery increases the availability of natriuretic peptides (NPR-A/NPR-C ratio: HFD + sham 0.2 ± 0.1 , HFD + RDN 3.6 ± 1.4 AU, $P = 0.05$; NPR-B/NPR-C ratio: HFD + sham 0.2 ± 0.1 , HFD + RDN 3.4 ± 1.4 AU, $P = 0.07$) (Fig. 5C) in the liver by reducing their clearance, further suggesting that RDN improves hepatic S_1 -activating pathways that downregulate hepatic GNG. Natriuretic peptides have been suggested to increase thermogenesis, especially in adipose tissue, by interacting with the SNS (19). Therefore, we studied the expression of ADRs in the liver. We found that RDN significantly reduced the expression of α -1A ADR (HFD + sham 0.5 ± 0.2 , HFD + RDN 0.1 ± 0.07 AU, $P = 0.04$) (Fig. 5D) in the liver, a $G_{q/11}$ -type G-protein-coupled receptor (GPCR) that has been shown to induce GNG gene expression in the liver (20). In sharp contrast to our expectation, we found significantly higher NE content in the livers of the RDN group compared with the sham group (Fig. 5E), suggesting a compensatory increase in hepatic SNS activity. This increase in hepatic NE content may explain the induction of gene expressions of both α -2A ADR (HFD + sham 0.2 ± 0.04 , HFD + RDN 1.4 ± 0.5 AU, $P = 0.02$) (Fig. 5D), a G_i -type GPCR (adenylyl cyclase inhibitor), and β -1 ADR (HFD + sham 1.0 ± 0.2 , HFD + RDN 2.9 ± 0.6 AU, $P = 0.013$) (Fig. 5D), a G_s -type GPCR (adenylyl cyclase stimulator) (21) in the liver with RDN. We found no changes in the catecholamine content in any other tissue (Supplementary Fig. 4). These results suggest that RDN improves hepatic S_1 through pathways that downregulate hepatic GNG genes.

Denervation Did Not Alter Kidney Function

Tests revealed no changes in urine chemistry, including osmolality, glucose, and lactate (Supplementary Fig. 5A–C), throughout the study in either the sham or the RDN group, suggesting that RDN did not impair renal function.

We found reduced gene expression of NPR-A and NPR-B in the kidney of RDN animals, suggesting a reduction in natriuresis to maintain normal kidney function and urine osmolality (Supplementary Fig. 5D and E). No signs of urinary tract infection were found.

DISCUSSION

The major new finding of this study is that effective surgical RDN totally reverses diet-induced hepatic insulin resistance and does so primarily by decreasing hepatic-specific GNG gene expression. By surgically transecting the main renal nerves under direct vision and painting the cut nerves with the neurotoxin phenol, we ensured extensive bilateral destruction of renal nerves, which was confirmed by an 80% reduction in renal tissue NE levels. That renal tissue EP levels also was decreased after RDN provides further proof for extensive renal nerve destruction. Circulating EP is taken up by postganglionic sympathetic nerve terminals, which were destroyed by RDN, and coreleased with NE during sympathetic nerve stimulation (22). We also demonstrate that basal and hypoglycemia-induced plasma EP response and renin activity are conserved after RDN surgery, suggesting an intact neural circuitry of the adrenals.

The seminal finding of this study is that effective RDN normalizes hepatic S_1 because it restored the impaired ability of insulin to suppress hepatic EGP despite continued exposure to HFD. These findings together with the further observation that RDN partially restored whole-body S_1 by minimal model assessment in the canine model of diet-induced obesity confirms and extends the uncontrolled clinical data solely based on the HOMA of insulin resistance index, which is limited because it does not accurately reflect changes in insulin resistance as previously shown (13).

The current data suggest that RDN normalizes hepatic S_1 by reducing the hepatic-specific expression of multiple GNG genes, including G6Pase, PEPCK, and transcription factors FOXO1, PGC-1 α , and PPAR- α . Insulin resistance previously has been characterized by increased hepatic expression of these genes (23,24). RDN surgery was accompanied by increased expression of LXR- α , a transcription factor regulator involved in the control of GNG genes through downregulation of PGC-1 α , G6Pase, and PEPCK (17). LXR- α also may interact with natriuretic peptides and ADRs (18,25). RDN surgery reduced the expression of NPR-C, suggesting increased natriuretic peptide content in the liver (19). Further studies are necessary to elucidate whether natriuretic peptides have a direct effect on hepatic glucose output and/or mediate the observed effects of renal nerves on hepatic gluconeogenesis.

Several observations implicate hepatic ADR mediation because RDN was accompanied by 1) increased hepatic NE content, suggesting increased hepatic SNA; 2) lower expression of the hepatic α -1A ADR, which is involved in upregulation of hepatic GNG genes through a $G_{q/11}$ GPCR pathway (20,26,27); and 3) increased expression of both hepatic α -2A ADR (G_i , adenylyl cyclase inhibitor) and

hepatic β -1 ADR (G_s , adenylyl cyclase stimulator). Diaz-Cruz et al. (28) demonstrated that activation of α -1 ADR inhibits β -ADR-stimulated pathways through NOX2 activation. Together, the current results suggest suppression of hepatic gluconeogenesis with RDN surgery through α -1 ADR, natriuretic peptides, and the LXR- α pathway. Further investigation is necessary to develop a complete picture of the mechanistic underpinnings.

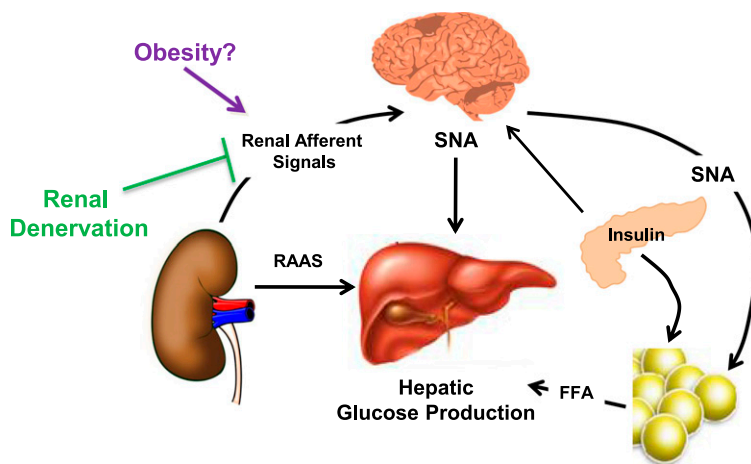
Lower GNG gene expression was not reflected by lower basal EGP but by insulin-mediated suppression of EGP. This is paradoxical because the tissue biopsy specimens were collected under fasting, noninsulin-stimulated conditions. Therefore, one would expect lower hepatic GNG gene expression with RDN to be reflected in lower basal EGP during EGC. However, we only found lower EGP under the insulin-stimulated condition during the clamp. Further studies investigating GNG protein expression, regulation, and activity as well as other pathways related to liver EGP, such as glycogen synthesis and breakdown, are required to understand this phenomenon.

RDN did not have an effect on peripheral S_I as measured by EGC, which is likely because 6 weeks of HFD feeding did not cause a significant impairment in peripheral S_I . Therefore, the current study could not detect a restoration in peripheral S_I . This is congruent with the catecholamine content in the peripheral tissues where we did not find significant differences in NE levels in the muscle and visceral and subcutaneous fat depots between the sham and RDN groups (Supplementary Fig. 4). In contrast to our findings, Rafiq et al. (29) observed an improvement in peripheral glucose disposal with RDN surgery in diabetic rats along with a lowering of blood pressure and suppression of SGLT2. However, whether the insulin-sensitizing effects observed by Rafiq et al. were independent or secondary to changes in cardiovascular factors is unclear.

We considered the possibility that RDN could potentially modulate hepatic EGP by decreasing plasma glucagon, the secretion of which can be decreased by central sympatholytic agents as well as ADR antagonists (30,31). However, this is not the case because plasma glucagon levels were unchanged with HFD alone or in combination with RDN (Supplementary Fig. 6).

Consistent with previously published data in canines (14), we did not find an effect of HFD on fasting glycemia (Supplementary Fig. 6A). Accompanying insulin resistance was apparently compensated for by fasting hyperinsulinemia (Supplementary Fig. 6C). However, RDN surgery had no effect on fasting glucose or hyperinsulinemia (Supplementary Fig. 6A and C) possibly due to reduced insulin clearance because fasting C-peptide levels were also not changed by surgery (Supplementary Fig. 6D), indicating a liver effect. The current fasting glycemia results are similar to those of a recent study in Norwegian subjects with hypertension and insulin resistance (32), which showed only a slight effect of catheter-based RDN on hepatic S_I with no measureable effect on fasting glucose. Also in this Norwegian study, the effects of RDN on hepatic S_I were lost at higher insulin doses, which may be due to the nature of the two-step clamp wherein the insulin dosage during the first step could potentially confound the results observed during the second step.

How does RDN suppress insulin-stimulated hepatic EGP? The direct versus indirect role of insulin in suppressing hepatic EGP has been under debate (33). We speculate that bilateral RDN suppresses the activity of both ERNs and ARNs, which in turn sensitize the liver glucose output to insulin possibly through central integration of inhibitory ARN signals or neurohormonal control of renin release and the angiotensin II and aldosterone system (Fig. 6). ARNs project centrally through the dorsal root ganglia to the nucleus of the solitary tract and evoke reflex changes in



Hypotheses: Indirect Regulation of Liver Glucose Production

Figure 6—Working hypotheses of indirect control of hepatic glucose production. Liver glucose output can be regulated indirectly by ARNs and ERNs by either central integration of ARN signals, central insulin signaling, adrenergic control of adipose tissue lipolysis, or neurogenic control of RAAS.

SNA to target tissues involved in blood pressure (34). Thus, the ARNs could potentially participate in central nervous system control of hepatic EGP by either reflex changes in hepatic SNA and vasculature, changes in central insulin signaling (35,36), activation of mediobasal hypothalamic K_{ATP} channels and the efferent hepatic branch of the vagal nerve (37), or ventromedial hypothalamus projections to the splanchnic sympathetic nerves that innervate the liver and control EGP (38,39). The central integration of ARN signals may also be involved in adrenergic control of adipose tissue lipolysis, which in turn may suppress hepatic EGP, conforming to the single gateway hypothesis proposed by our group after experimentally demonstrating that suppression of hepatic EGP is indirectly mediated by suppression of visceral fat lipolysis by insulin (40–42). Another possible hypothesis is that RDN suppresses the systemic renin-angiotensin-aldosterone system (RAAS), improving peripheral glucose metabolism; however, the effects of RAAS on glucose metabolism are believed to be mainly hemodynamic (43,44). We do not expect changes in angiotensin II or aldosterone regulation to have a large effect on glucose metabolism because in clinical trials, ACE inhibitors and angiotensin receptor blockers have had meager, if any, effects on impaired glucose metabolism (45,46). Further investigation is necessary to illuminate these pathways.

This study has potential limitations. We did not measure arteriovenous difference across the kidney to quantify changes in net renal EGP or renal NE spillover with RDN. We also did not directly measure the effect of RDN on in vivo gluconeogenesis using labeled substrate such as lactate and alanine and in vitro hepatic gluconeogenesis. Measurement of in vivo transhepatic GNG substrate turnover requires catheterization of the hepatic and portal veins (47), which was not technically feasible. Our hepatic GNG gene expression data only suggest that the liver is the primary effector site of changes in glucose metabolism induced by renal nerve ablation. Further investigation is necessary to establish the molecular pathways involved, including protein levels and signaling through insulin and other pathways that can contribute to changes in liver glucose metabolism. We do not have a direct physiological measurement of local or whole-body SNA. However, there are no methods currently available that directly measure SNA (48,49). Because we did not measure hepatic SNA, we do not know whether the increased hepatic NE content was due to increased SNA, decreased clearance, or both. We also have not established the exact neural or hormonal circuitry involved in eliciting a hepatic response to RDN; however, future studies will address this. Because the postsurgery follow-up period was rather short in the current design, long-term studies are needed to determine whether the marked effects are sustained or permanent.

With this dog study, we were able to overcome some of the key limitations of clinical trials, including direct open surgical denervation and renal NE content to prove that we in fact ablated the nerves. Direct validation of successful RDN is technically difficult to perform in humans but essential to draw inferences from clinical trials. We cannot

rule out species differences between canines and humans as a factor contributing to the results. From the perspective of potential clinical translation, a future study to determine whether the canine results can be repeated in humans would be important. That the RDN animals demonstrated resistance to insulin-induced hypoglycemia also is noteworthy, suggesting the involvement of renal sympathetic nerves in the hypoglycemic counterregulatory circuit that is perhaps mediated through the liver, a potential clinical application of RDN in hypoglycemia management in patients with diabetes. The results suggest that RDN improves insulin resistance and could thus be used to treat human diabetes and comorbidities such as cardiovascular disease, which affects 8.3% of the global population (50).

In conclusion, bilateral RDN improved S_I in diet-induced insulin resistance mainly by improving hepatic S_I , supporting a novel crosstalk between the renal nerves and the liver. The translational potential of this work to the clinical setting will be fascinating to investigate.

Acknowledgments. The authors thank Rita Thomas, Hasmik Mkrtchyan, Edgardo Paredes, Jorge Giani, Chun-I Yang, and the comparative medicine staff at Cedars-Sinai Medical Center for technical assistance.

Funding. This work was supported by the National Institutes of Health National Institute of Diabetes and Digestive and Kidney Diseases grants DK-27619 and DK-29867 to R.N.B.

Duality of Interest. No potential conflicts of interest relevant to this article were reported.

Author Contributions. M.S.I. contributed to the study concept and design, molecular biology experimental concept and design, experiments, data analysis, results interpretation, preparation of figures, and writing and revision of the manuscript. R.N.B. contributed to the study concept and design, results interpretation, and revision of the manuscript. J.E.K. contributed to the surgeries and revision of the manuscript. O.O.W. contributed to the surgeries, experiments, and revision of the manuscript. M.K. contributed to the molecular biology experimental concept and design and results interpretation. R.G.V. contributed the study concept and design and revision of the manuscript. D.J.C. contributed to the molecular biology experimental concept and design. C.K. contributed to the study concept and design, experiments, results interpretation, and revision of the manuscript. M.S.I. is the guarantor of this work and, as such, had full access to all the data in the study and takes responsibility for the integrity of the data and the accuracy of the data analysis.

Prior Presentation. Parts of this study were presented in abstract form at the 76th Scientific Sessions of the American Diabetes Association, New Orleans, LA, 10–14 June 2016; 75th Scientific Sessions of the American Diabetes Association, Boston, MA, 5–9 June 2015; Obesity Society Annual Scientific Meeting, Los Angeles, CA, 2–7 November 2015; Endocrine Society's 97th Annual Meeting and Expo, San Diego, CA, 5–8 March 2015; and 15th Annual Rachmiel Levine Diabetes and Obesity Symposium, San Diego, CA, 1–4 March 2015.

References

1. Krum H, Schlaich M, Whitbourn R, et al. Catheter-based renal sympathetic denervation for resistant hypertension: a multicentre safety and proof-of-principle cohort study. *Lancet* 2009;373:1275–1281
2. Mahfoud F, Schlaich M, Kindermann I, et al. Effect of renal sympathetic denervation on glucose metabolism in patients with resistant hypertension: a pilot study. *Circulation* 2011;123:1940–1946
3. Dibona GF. The functions of the renal nerves. In: *Reviews of Physiology, Biochemistry and Pharmacology*. Vol. 94. Adrian RH, zur Hausen H, Helmreich E, et al., Eds. New York, Springer-Verlag, 1982, p. 75–181

4. Recordati G, Moss NG, Genovesi S, Rogenes P. Renal chemoreceptors. *J Auton Nerv Syst* 1981;3:237–251
5. Hall JE, do Carmo JM, da Silva AA, Wang Z, Hall ME. Obesity-induced hypertension: interaction of neurohumoral and renal mechanisms. *Circ Res* 2015;116:991–1006
6. Converse RL Jr, Jacobsen TN, Toto RD, et al. Sympathetic overactivity in patients with chronic renal failure. *N Engl J Med* 1992;327:1912–1918
7. Bhatt DL, Kandzari DE, O'Neill WW, et al.; SYMPLICITY HTN-3 Investigators. A controlled trial of renal denervation for resistant hypertension. *N Engl J Med* 2014;370:1393–1401
8. Schlaich MP, Straznicki N, Grima M, et al. Renal denervation: a potential new treatment modality for polycystic ovary syndrome? *J Hypertens* 2011;29:991–996
9. Witkowski A, Prejzisz A, Florczak E, et al. Effects of renal sympathetic denervation on blood pressure, sleep apnea course, and glycemic control in patients with resistant hypertension and sleep apnea. *Hypertension* 2011;58:559–565
10. Denker MG, Cohen DL, Townsend RR. Catheter-based renal artery denervation for resistant hypertension: promise unfulfilled or unsettled? *Curr Atheroscler Rep* 2015;17:56
11. Pekarskiy S, Baev A, Mordovin V, et al. Failure of renal denervation in SYMPLICITY HTN-3 is a predictable result of anatomically inadequate operative technique and not true limitations of the technology. *J Hypertens* 2015;33(Suppl. 1):e108
12. Kim SP, Catalano KJ, Hsu IR, Chiu JD, Richey JM, Bergman RN. Nocturnal free fatty acids are uniquely elevated in the longitudinal development of diet-induced insulin resistance and hyperinsulinemia. *Am J Physiol Endocrinol Metab* 2007;292:E1590–E1598
13. Ader M, Stefanovski D, Richey JM, et al. Failure of homeostatic model assessment of insulin resistance to detect marked diet-induced insulin resistance in dogs. *Diabetes* 2014;63:1914–1919
14. Ader M, Stefanovski D, Kim SP, et al. Hepatic insulin clearance is the primary determinant of insulin sensitivity in the normal dog. *Obesity (Silver Spring)* 2014;22:1238–1245
15. Ganong WF. Sympathetic effects on renin secretion: mechanism and physiological role [Internet], 1972. New York, Springer. Available from http://link.springer.com/chapter/10.1007/978-1-4684-0940-6_2. Accessed 2 October 2015
16. Otsuka K, Assaykeen TA, Goldfien A, Ganong WF. Effect of hypoglycemia on plasma renin activity in dogs. *Endocrinology* 1970;87:1306–1317
17. Laffitte BA, Chao LC, Li J, et al. Activation of liver X receptor improves glucose tolerance through coordinate regulation of glucose metabolism in liver and adipose tissue. *Proc Natl Acad Sci U S A* 2003;100:5419–5424
18. Cannon MV, Silljé HHW, Sijbesma JWA, et al. LXR α improves myocardial glucose tolerance and reduces cardiac hypertrophy in a mouse model of obesity-induced type 2 diabetes. *Diabetologia* 2016;59:634–643
19. Palmer BF, Clegg DJ. An emerging role of natriuretic peptides: igniting the fat furnace to fuel and warm the heart. *Mayo Clin Proc* 2015;90:1666–1678
20. Exton JH. Mechanisms involved in alpha-adrenergic phenomena: role of calcium ions in actions of catecholamines in liver and other tissues. *Am J Physiol* 1980;238:E3–E12
21. Zhong H, Minneman KP. Alpha1-adrenoceptor subtypes. *Eur J Pharmacol* 1999;375:261–276
22. Berecek KH, Brody MJ. Evidence for a neurotransmitter role for epinephrine derived from the adrenal medulla. *Am J Physiol* 1982;242:H593–H601
23. Michael MD, Kulkarni RN, Postic C, et al. Loss of insulin signaling in hepatocytes leads to severe insulin resistance and progressive hepatic dysfunction. *Mol Cell* 2000;6:87–97
24. Saltiel AR, Kahn CR. Insulin signalling and the regulation of glucose and lipid metabolism. *Nature* 2001;414:799–806
25. Merkulov VM, Merkulova TI. Structural variants of glucocorticoid receptor binding sites and different versions of positive glucocorticoid responsive elements: analysis of GR-TRRD database. *J Steroid Biochem Mol Biol* 2009;115:1–8
26. Exton JH, Mallette LE, Jefferson LS, et al. The hormonal control of hepatic gluconeogenesis. *Recent Prog Horm Res* 1970;26:411–461
27. Han C, Bowen WC, Michalopoulos GK, Wu T. Alpha-1 adrenergic receptor transactivates signal transducer and activator of transcription-3 (Stat3) through activation of Src and epidermal growth factor receptor (EGFR) in hepatocytes. *J Cell Physiol* 2008;216:486–497
28. Diaz-Cruz A, Vilchis-Landeros MM, Guinzberg R, Villalobos-Molina R, Piña E. NOX2 activated by α 1-adrenoceptors modulates hepatic metabolic routes stimulated by β -adrenoceptors. *Free Radic Res* 2011;45:1366–1378
29. Rafiq K, Fujisawa Y, Sherajee SJ, et al. Role of the renal sympathetic nerve in renal glucose metabolism during the development of type 2 diabetes in rats. *Diabetologia* 2015;58:2885–2898
30. Yakubu-Madus FE, Johnson WT, Zimmerman KM, Dananberg J, Steinberg MI. Metabolic and hemodynamic effects of moxonidine in the Zucker diabetic fatty rat model of type 2 diabetes. *Diabetes* 1999;48:1093–1100
31. Ahrén B, Lundquist I. Alpha-adrenoceptor blockade by phentolamine inhibits beta-adrenergically and cholinergically induced glucagon secretion in the mouse. *Horm Metab Res* 1987;19:600–603
32. Miroslawska AK, Gjessing PF, Solbu MD, Fuskevåg OM, Jenssen TG, Steigen TK. Renal denervation for resistant hypertension fails to improve insulin resistance as assessed by hyperinsulinemic-euglycemic step clamp. *Diabetes* 2016;65:2164–2168
33. Bergman RN. New concepts in extracellular signaling for insulin action: the single gateway hypothesis. *Recent Prog Horm Res* 1997;52:359–385; discussion 385–387
34. Ciriello J, Calaresu FR. Hypothalamic projections of renal afferent nerves in the cat. *Can J Physiol Pharmacol* 1980;58:574–576
35. Obici S, Zhang BB, Karkanias G, Rossetti L. Hypothalamic insulin signaling is required for inhibition of glucose production. *Nat Med* 2002;8:1376–1382
36. Rojas JM, Schwartz MW. Control of hepatic glucose metabolism by islet and brain. *Diabetes Obes Metab* 2014;16(Suppl. 1):33–40
37. Pocai A, Lam TKT, Gutierrez-Juarez R, et al. Hypothalamic K(ATP) channels control hepatic glucose production. *Nature* 2005;434:1026–1031
38. Hartmann H, Beckh K, Jungermann K. Direct control of glycogen metabolism in the perfused rat liver by the sympathetic innervation. *Eur J Biochem* 1982;123:521–526
39. Shimazu T. Innervation of the liver and gluco-regulation: roles of the hypothalamus and autonomic nerves. *Nutrition* 1996;12:65–66
40. Ader M, Bergman RN. Peripheral effects of insulin dominate suppression of fasting hepatic glucose production. *Am J Physiol* 1990;258:E1020–E1032
41. Bergman RN. Non-esterified fatty acids and the liver: why is insulin secreted into the portal vein? *Diabetologia* 2000;43:946–952
42. Mittelman SD, Bergman RN. Inhibition of lipolysis causes suppression of endogenous glucose production independent of changes in insulin. *Am J Physiol Endocrinol Metab* 2000;279:E630–E637
43. Henriksen EJ, Jacob S, Kinnick TR, Youngblood EB, Schmit MB, Dietze GJ. ACE inhibition and glucose transport in insulin resistant muscle: roles of bradykinin and nitric oxide. *Am J Physiol* 1999;277:R332–R336
44. Berne C, Pollare T, Lithell H. Effects of antihypertensive treatment on insulin sensitivity with special reference to ACE inhibitors. *Diabetes Care* 1991;14(Suppl. 4):39–47
45. Seefeldt T, Ørskov L, Mengel A, et al. Lack of effects of angiotensin-converting enzyme (ACE)-inhibitors on glucose metabolism in type 1 diabetes. *Diabet Med* 1990;7:700–704
46. Abuissa H, Jones PG, Marso SP, O'Keefe JH Jr. Angiotensin-converting enzyme inhibitors or angiotensin receptor blockers for prevention of type 2 diabetes: a meta-analysis of randomized clinical trials. *J Am Coll Cardiol* 2005;46:821–826
47. Cherrington AD, Fuchs H, Stevenson RW, Williams PE, Alberti KG, Steiner KE. Effect of epinephrine on glycogenolysis and gluconeogenesis in conscious overnight-fasted dogs. *Am J Physiol* 1984;247:E137–E144
48. Grassi G, Esler M. How to assess sympathetic activity in humans. *J Hypertens* 1999;17:719–734
49. Lansdown A, Rees DA. The sympathetic nervous system in polycystic ovary syndrome: a novel therapeutic target? *Clin Endocrinol (Oxf)* 2012;77:791–801
50. Whiting DR, Guariguata L, Weil C, Shaw J. IDF diabetes atlas: global estimates of the prevalence of diabetes for 2011 and 2030. *Diabetes Res Clin Pract* 2011;94:311–321